Talanta 246 (2022) 123526

Contents lists available at ScienceDirect

Talanta

journal homepage: www.elsevier.com/locate/talanta

Assisting dementia diagnosis through the electrochemical immunosensing of glial fibrillary acidic protein

Goksu Ozcelikay [a,b], María Gamella [b], Mehmet Altay Unal [c], Kıvılcım Gucuyener [d], Ana Montero-Calle [e], Rodrigo Barderas [e], José M. Pingarrón [b], Susana Campuzano [b,**], Sibel A. Ozkan [a,*]

[a] Ankara University, Faculty of Pharmacy, Department of Analytical Chemistry, 06560, Ankara, Turkey
[b] Department of Analytical Chemistry, Faculty of Chemistry, Complutense University of Madrid, 28014, Madrid, Spain
[c] Ankara University, Stem Cell Institute, 06520, Ankara, Turkey
[d] Gazi University, Faculty of Medicine, Department of Pediatric Neurology, 06510, Ankara, Turkey
[e] Chronic Disease Programme, UFIEC, Institute of Health Carlos III, Majadahonda, 28220, Madrid, Spain

ARTICLE INFO

Keywords:
GFAP
Immunoplatform
Alzheimer disease
MBs
Brain tissue extracts

ABSTRACT

Glial fibrillary acidic protein (GFAP) is a member of the intermediate filament family of proteins with increased levels in serum and cerebrospinal fluid of patients with Alzheimer disease (AD) and other neurodegenerative diseases (NDs), such as vascular dementia (VD). This work describes the first magnetic microbeads (MBs)-based electrochemical immunoplatform for GFAP determination. The platform design comprises a sandwich immunoassay implemented on the MBs surface and amperometric transduction at single-use screen-printed carbon electrodes (SPCEs). Micro-sized carboxylic acid magnetic particles (COOH-MBs) were modified with a specific capture antibody (CAb) to selectively link the target protein, which was sandwiched with a biotinylated detector antibody (btn-DAb) further conjugated with a streptavidin-peroxidase (Strep-HRP) conjugate. Amperometric transduction was performed at SPCEs upon capturing the magnetic bioconjugates on their surface and through the hydrogen peroxide/hydroquinone (H_2O_2/HQ) system. The immunoplatform achieved a limit of detection of 67 pg mL^{-1} for the amperometric detection of standards and selectivity compatible with clinical applicability to assist in minimally invasive NDs diagnosis and prognosis. The MBs-based immunoplatform was applied with good results to determine the endogenous content of GFAP in protein brain extracts without matrix effect and using just 6.25 ng of sample per determination. Furthermore, the developed methodology was capable of differentiating between healthy subjects and patients diagnosed with VD and AD in only 2 h, providing accurate results in line with those obtained by an ELISA kit that used the same immunoreagents.

1. Introduction

Accurate diagnosis of neurodegenerative diseases (NDs) is a matter of intense research. Among NDs, Alzheimer's disease (AD) and vascular dementia (VD) are the prevalent cause of cognitive impairment among the elderly. Histopathologically, AD can be identified by the extracellular amyloid-β (Aβ) plaques formation and by the presence of abnormally phosphorylated tau protein producing intracellular neuronal tangles in the brain [1]. In addition, several studies confirmed overlapping between AD and VD, and thus classical neuropathological changes of AD (plaques and tangles) can be observed in VD [2] Even though post-mortem identification of these hallmarks is required for as diagnostic confirmation, clinical assessment of these diseases is aided by the in-life determination of validated biomarkers using positron emission tomography (PET) and cerebrospinal fluid (CSF) analysis [3,4]. Besides, the cost of PET imaging and the invasiveness of lumbar puncture make it difficult to use these methods in standard clinical practice [5,6]. In this sense, the less-invasive nature of blood-based biomarkers is an interesting alternative for the initial clinical diagnostic testing. Although phosphorylated tau species [7,8] and Aβ 42/40 ratio [9] are promising blood biomarkers for detecting AD, other blood biomarkers can help to improve accuracy in diagnosing dementia during life.

* Corresponding author.
** Corresponding author.
E-mail addresses: susanacr@quim.ucm.es (S. Campuzano), sibel.ozkan@pharmacy.ankara.edu.tr (S.A. Ozkan).

https://doi.org/10.1016/j.talanta.2022.123526
Received 2 February 2022; Received in revised form 10 March 2022; Accepted 1 May 2022
Available online 5 May 2022
0039-9140/© 2022 Elsevier B.V. All rights reserved.

NDs are related to the molecular, morphologic, and functional remodeling of astrocytes, a process which is known as reactive astrogliosis [10]. Astrocytes are glial cells associated with modulation of synapses, homeostasis, transport of nutrients, brain signaling, and structural support [1]. When some type of brain damage occurs, a reaction of the astroglia cells takes place, the so-called astrogliosis, which tries to contain the brain damage by elevating the expression of specific markers. Indeed, astrogliosis is a common neuropathological finding in brain disorders such as AD, VD, and *frontotemporal dementia* (FTD) [11]. Several studies have demonstrated that astrogliosis is an early characteristic in the pathological progression of AD, whose decrease over the development of the disease is contrary to the increase in Aβ plaque load [6]. Nevertheless, few astrocyte fluid biomarkers have been investigated so far [12]. Astrogliosis is often manifested by elevated levels of glial fibrillary acidic protein (GFAP) expression [13], the main protein constituent of intermediate filaments of astrocytes [10], and specific to brain tissue. It is released into the interstitial fluid only after astrocytes death [14], and subsequently it intrudes the bloodstream by penetrating the blood-brain barrier [15]. Indeed, GFAP is a usually measured biomarker in CSF after a lumbar puncture of the patient and found to be elevated in AD and VD patients [16,17]. Current findings claim that GFAP measurement in blood plasma is better than in CSF for accurately and less invasive identification of the AD stage the affected person might be in [12]. Indeed, it has been shown that elevated plasma GFAP concentration can be found at the early stages of AD and increase during the disease progression, which makes it a particularly promising biomarker for early-stage and minimally invasive AD diagnosis [4,12].

Among the available methods for detecting NDs biomarkers, biosensors, especially electrochemical biosensors, stand up as an interesting choice due to their high sensitivity, low cost, simple handling, fast response, and in-field operation. The electrochemical immunosensors described until now for the determination of GFAP [18–21] have proven to be competitive biotools compared to the conventional methodologies used in centralized laboratories, such as enzyme-linked immunosorbent assays (ELISA), immunohistochemistry and Western blot assays [16, 22–25], which require relatively expensive and hardly portable instrumentation. Although the reported electrochemical immunosensors achieved a single-digit pg mL^{-1} sensitivity, they were implemented for the protein analysis in spiked serum [19] and plasma [21] samples, but they did not demonstrate real-world applicability to distinguish between healthy individuals and diseased patients.

In response to the need for improved tests for NDs diagnosis and given the unique attributes of electrochemical biosensors coupled with magnetic microbeads (MBs), we describe here the first MBs-based amperometric immunosensor for the sensitive analysis of GFAP involving a simple approach. A specific GFAP capture antibody (CAb) was covalently immobilized to carboxylated magnetic microbeads (COOH-MBs) to perform a sandwich-type assay. Once GFAP was captured by the CAb-MBs immunoconjugates, a biotin-modified detector antibody (btn-DAb) recognized GFAP, leading to a sandwich immunoconjugate which was tagged with a streptavidin horseradish peroxidase (Strep-HRP) conjugate. GFAP was electrochemically interrogated through the H_2O_2/HQ system. The reported immunoplatform showed its effectiveness for accurately determining the endogenous GFAP content in brain protein extract samples from healthy individuals and NDs patients, using only 6.25 ng of the raw protein extract, in just 2 h.

2. Experimental section

Used apparatus, electrodes, reagents, and solutions are defined detailly in the supplementary information.

2.1. Bio-functionalization of MBs

An aliquot of 3 μL of the commercial COOH-MBs suspension was added into a 1.5 mL microcentrifuge tube and rinsed twice with 50 μL of 0.025 M MES buffer in the thermo-shaker for 10 min (25 °C, 950 rpm). The MBs were magnetically captured by means of a magnet for 3 min to remove the supernatant in all the required steps. The COOH-MBs surface was activated in a freshly prepared EDC/sulfo-NHS solution (25 μL) upon incubation for 35 min in the thermo-shaker (950 rpm, 25 °C). Once activated, the COOH-MBs were washed twice with 0.025 MES (50 μL) and re-suspended in 25 μL of 25 μg mL^{-1} CAb solution made in 0.025 μM MES (pH 5.0) to incubate at 25 °C under constant stirring (950 rpm) for 15 min to perform the covalent binding of the CAb onto COOH-MBs. The modified CAb–COOH–MBs were rinsed twice with 0.025 MES (50 μL) and the unreacted groups blocked with 1 M ethanolamine prepared in phosphate solution (pH 8.0) through incubation for 60 min (25 °C, 950 rpm). The as-modified MBs were then rinsed with 50 μL of 0.1 M TRIS–buffer (pH 7.2) and further twice with 50 μL of PBS (pH 7.4). The obtained CAb–COOH–MBs were re-suspended in sterilized PBS buffer solution and stored at 4 °C until use.

2.2. Sandwich immunoassay onto the MBs

The immunoassay protocol consisted of two steps: incubation of the modified CAb–COOH–MBs in 25 μL of a solution containing a mixture of GFAP standards (or the tested sample) and 0.25 μg mL^{-1} btn-DAb solution (made in BB) for 60 min (25 °C, 950 rpm) and incubation of the btn-DAb-GFAP-CAb–COOH–MBs in a 1/250 dilution of Strep-HRP solution (prepared in BB) for 60 min (25 °C, 950 rpm). The modified MBs were rinsed twice with 50 μL of BB solution after each step. The MBs bearing the sandwich immunoconjugates (HRP-Strep-btn-DAb-GFAP-CAb-MB–COOH–MBs) were re-suspended in 50 μL of 0.05 M phosphate buffer (pH 6.0) to realize the amperometric measurements.

2.3. Amperometric detection

The MBs suspension was carefully pipetted on a SPCE previously settled in the home-made poly(methyl methacrylate (PMMA) holder with a Nd magnet. The MBs-modified SPCE-holder was placed into an electrochemical cell which contained 10 mL of 0.05 M phosphate buffer (pH 6.0) in the presence of fresh 1.0 mM HQ solution [26]. Amperometric measurements in stirring conditions were carried out by applying a detection potential of −0.20 V *vs.* the Ag pseudoreference electrode. When background current became steady, 50 μL of a 0.1 M fresh H_2O_2 solution were pipetted into the electrochemical cell and the cathodic current arising from the enzymatic reduction of H_2O_2 mediated by HQ [27] was recorded. The provided signals correspond to the variation between the steady-state and the background current, and the figures are calculated as the mean of three replicates, which were used to estimate the error bars as the triple of the standard deviation for each set of replicates ($\alpha = 0.05$).

2.4. Analysis of protein brain tissue extracts

The analyzed samples of brain tissue with indicated pathological conditions were obtained from the CIEN Foundation's Tissue Bank (BT-CIEN). Pathological conditions were confirmed post-mortem according to the international consensus criteria [28]. In brief, in all cases, post-mortem examination was limited to the cranial cavity, according to the brain bank protocol. Neuropathological classification was based on the examination of hematoxylin and eosin-stained paraffin sections of all blocks and immunostaining with a panel of antibodies (Aβ, tau AT100, α-synuclein, ubiquitin, and TDP-43) and myelin stain. Consensus criteria were used for disease diagnosis and staging. Alzheimer's type changes were assessed following NIAAA guidelines [28]. The BT-CIEN develops a brain donation program based on standard operating procedures (SOPs), meeting the ethical and legal requirements established by current legislation regarding the protection of personal data and the use of human origin samples for biomedical research. Written informed

consent was obtained from all individuals.

Brain tissue protein extraction was made according to the established protocol [29,30]. Briefly, tissue samples were chopped in small pieces using dry ice, mechanically disaggregated with 0.5% SDS in PBS with a protease inhibitor cocktail (Sigma). Finally, they were clarified by centrifuging at 10,000 rpm. The obtained brain tissue protein extracts were kept at −80 °C until use. Protein extracts quality was assessed prior to be used by Coomassie staining of SDS-PAGE 10% gels [31].

The determination was conducted using 6.25 ng of crude tissue extract, without further sample treatment, following the protocols written in sections 2.4 and 2.5. Due to the absence of matrix effect with such amount of lysate, the endogenous GFAP concentration was quantified by interpolating the current measured for the samples into the calibration graph built with GFAP standard solutions.

The results were compared to those obtained by using the ELISA method involving the same immunoreagents and using the protocol reported by Muñoz et al. [26]. The following concentrations of the reagents were employed: 4.0 μg mL^{-1} CAb solution (prepared in PBS), GFAP standard solutions or brain tissue extract sample (6.25 ng, made in Reagent Diluent solution), 40 ng mL^{-1} btn-DAb solution (in Reagent Diluent solution) and 1/40 Strep-HRP-diluted solution in Reagent Diluent solution. The determination of GFAP was carried out thorough the interpolation of the optical density measured for 80-times diluted samples between the linearity range built with standards over the 0–25 ng mL^{-1} range.

3. Results and discussion

Fig. 1 depicts a scheme of the developed electrochemical immunoplatform involving the use of magnetic microcarriers to carry out the immunoassay. The method relies on a sandwich-type immunoassay using COOH-MBs covalently modified with a GFAP specific CAb. The captured target protein is then sandwiched by btn-DAbs which were tagged with a Strep-HRP conjugate. The as modified MBs where magnetically captured on the SPCE surface by using a magnet, and the amperometric readout was carried out through the enzymatic reduction of H_2O_2 using HQ (as redox mediator) at −0.20 V *vs.* an Ag pseudoreference electrode, providing an increase in the cathodic current directly proportional to GFAP concentration.

3.1. Optimization of the experimental variables

The effect of experimental variables such as the CAb concentration, the incubation time for the CAb immobilization, the number of incubation steps concerning the sandwich immunoassay, the incubation time of the GFAP and btn-DAb mixture solution, the btn-DAb concentration, the Strep-HRP dilution and the corresponding incubation time, on the amperometric readouts provided by the immunoplatform were tested by calculating the ratio between the current measured in the presence (S) of 31.6 ng mL^{-1} GFAP standard solution and that measured in the absence of target protein (B), S/B ratio. The used supporting electrolyte and the pH value, as well as the H_2O_2 and HQ concentrations and the applied detection potential, were described in previous works [32,33]. The tested ranges for these experimental parameters and the optimal value for each parameter are reported in Table 1.

The influence of the CAb concentration on the immunoscaffold performance was assessed over the 0–50 μg mL^{-1} concentration range (Figure S1a in the Supporting Information). The S/B ratio raised with the CAb concentration until 25 μg mL^{-1} and remained practically constant for more concentrated CAb solutions, mainly due to the sterically

Table 1
Optimization of working parameters affecting the response of the developed MBs-based immunosensor for the amperometric assay of GFAP.

Variable	Checked range	Selected value
CAb concentration, μg mL^{-1}	0–50	25
Incubation time of CAb, min	15–90	15
Number of incubation steps	1–4	3
Incubation time for GFAP/btn-DAb mixture, min	15–120	60
btn-DAb concentration, μg mL^{-1}	0.1–1.0	0.25
Strep-HRP, dilution	1/50−1/2500	1/250
Incubation time of Strep-HRP, min	15–120	60

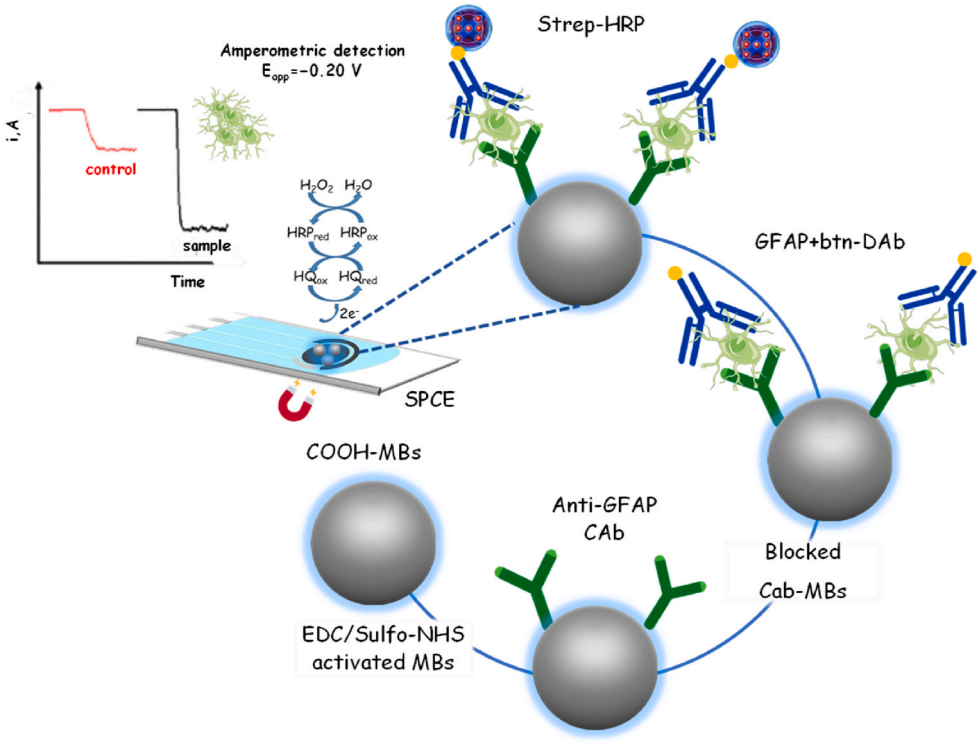


Fig. 1. Schematic display of the MBs-assisted immunoplatform preparation for the amperometric assay of GFAP.

hindrance effects in target binding when large antibody amounts on the MBs are immobilized on the surface [34]. As expected according to the immunoassay rationale, it was not possible to detect GFAP when no CAb was immobilized on the MBs (bars at 0 in Figure S1a). The incubation time for CAb immobilization was tested by incubating the activated COOH-MBs in CAb solution between 15 and 90 min (25 °C, 950 rpm). A better S/B ratio was reached for 15 min (Figure S1b). The high B signals obtained when low concentrations of CAb are immobilized (Figure S1a) or short incubation times are used for its immobilization (Figure S1b) could be due to nonspecific adsorptions of btn-DAb on MBs or on CAb. Different immunoassay protocols (summarized in Table 2) were evaluated by testing the number of involved incubation steps. All the assayed protocols consisted of incubating the CAb-MBs immunoconjugates in solutions containing the immunoreagents for 30 min. In the view of the results shown in Figure S1c, the protocol 2B involving two sequential incubation steps the CAb immunoconjugates, first in a GFAP/btn-DAb mixture solution and second in the Strep-HRP conjugate solution, provided larger S/B ratio, and, therefore, it was selected to develop the immunoplatform. Furthermore, an incubation time of 60 min with the GFAP/btn-DAb mixture solution was chosen for further work (Figure S1d). The influence of the btn-DAb concentration on the amperometric readouts was tested over the 0.1–1.0 μg mL^{-1} concentration range (Figure S1e). The S/B ratio raised with the btn-DAb concentration up to 0.25 μg mL^{-1} and dropped for larger concentrations regardless the specific current increase, due to the relatively larger increase of the non-specific current. Thus, 0.25 μg mL^{-1} was chosen as optimum. The effect of different Strep-HRP conjugate dilutions between 1/2500 and 1/100 was checked. A large dilution provoked a poorer discrimination (low S/B ratios), while a low dilution caused large non-specific adsorptions, and thus low S/B ratios (Figure S1f). Therefore, an intermediate 1/250 dilution was selected. Moreover, results in Figure S1g led us to select 60 min as incubation time for Strep-HRP.

3.2. Analytical performance of the immunoplatform for the amperometric determination of GFAP

A linear calibration plot ($R^2 = 0.998$) between the obtained cathodic current and the GFAP standard concentration was observed over the 0.24–31.6 ng mL^{-1} range (Fig. 2) obtaining slope and intercept values of (45 ± 2) nA mL ng^{-1} and (114 ± 28) nA, respectively. The limits of detection (LOD) and quantification (LQ) were calculated to meet the $3 \times s_b/m$ and $10 \times s_b/m$ criteria, respectively, where the standard deviation was calculated for 10 amperometric readings in the absence of GFAP (s_b) and m *is* the slope of the linear regression. Accordingly, the obtained LOD and LQ values were 67 pg mL^{-1} and 203 pg mL^{-1}, respectively. The achieved sensitivity not sufficient to discriminate Mild Cognitive Impairment (MCI)-AD status for which a cut-off value of 54.1 pg mL^{-1} in plasma has been established [6]. However, the immunoplatform allows discrimination of this type of patients by analyzing CSF where concentrations above 1 ng mL^{-1} have been reported [35]. It is noteworthy that the reached LOD is about six times smaller than the cut-off value found for GFAP in serum from traumatic brain injury (TBI) patients (1.5 μg mL^{-1}) [36].

Table 2
Protocols involving different numbers of the incubation steps, checked to develop the immunoplatform for GFAP determination.

Protocol	Steps (30 min incubation time each)
1	i. Mixture solution containing GFAP +0.5 μg mL^{-1} btn-DAb + 1/1000 diluted Strep-HRP
2A	i. GFAP ii. Mixture solution containing 0.5 μg mL^{-1} btn-DAb + 1/1000 diluted Strep-HRP
2B	i. Mixture solution containing GFAP+0.5 μg mL^{-1} btn-DAb ii. 1/1000 diluted Strep-HRP
3	i. GFAP ii. 0.5 μg mL^{-1} btn-DAb iii. 1/1000 diluted Strep-HRP

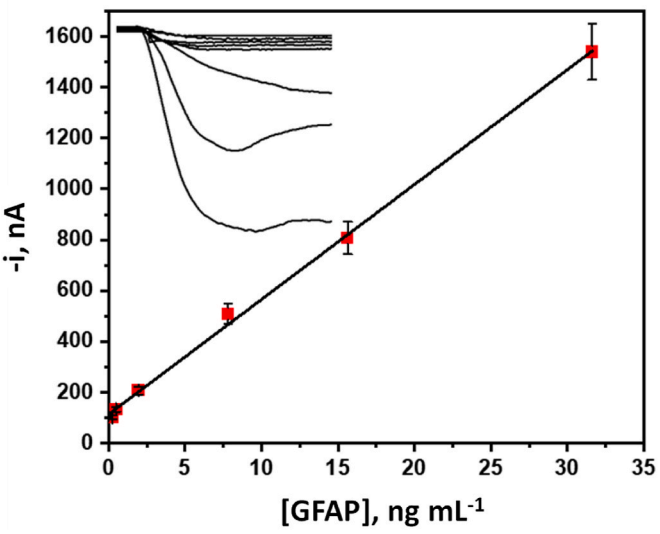


Fig. 2. Calibration curve obtained using the developed immunoplatform for the amperometric determination of GFAP. Inset: amperometric responses recorded for GFAP standards of different concentration (0, 0.244, 0.486, 1.95, 7.81, 15.6 and 31.6 ng mL^{-1}).

The reproducibility of the methodology was checked through the relative standard deviation (RSD) value obtained from the amperometric measurements of 7 different immunoplatforms made in the same manner on the same day for 7.8 ng mL^{-1} GFAP. The obtained RSD value, 8.2%, confirmed the acceptable reproducibility of the complete experimental procedure, including both the modification of the MBs with the immune complexes and the amperometric recordings obtained after their capture on the surface of the SPCE working electrode.

The storage stability of the CAb–COOH–MBs immunoconjugates was assessed upon keeping them in 0.01 mol L^{-1} PBS of pH 7.5 at 4 °C. No significant differences in terms of the measured S/B ratio value were found for the amperometric signals recorded with the stored CAb–COOH–MBs immunoconjugates for 0 and 7.8 ng mL^{-1} GFAP for at least 12 days (Figure S2 in the Supporting Information), thus allowing the immunoconjugate preparation in advance and their use when needed leading to less time-consuming determinations.

Other reported electrochemical sensors for the determination of GFAP are the following. Wang et al. [37] reported an electrochemical sensor involving molecularly-imprinted-polymer (MIP) technology and reaching a LOD of 0.04 μg mL^{-1} for standard GFAP solutions. Moreover, electrodes modified with dithiobis(succinimidyl propionate) self-assembled monolayers were employed for the covalent immobilization of anti-GFAP CAb and used for the label-free impedimetric detection of GFAP over the 1 pg mL^{-1} to 100 ng mL^{-1} concentration range with a LOD value of 1 pg mL^{-1} [18]. Khetani et al. reported an impedimetric immunosensor using polyethylenimine coated graphene screen-printed electrode, obtaining a linear range of 1 pg mL^{-1} to 100 ng mL^{-1} for GFAP [19]. Furthermore, the on-site GFAP determination was carried out in microcentrifuge tubes utilized as disposable immunoelectrochemical cells, it being possible to differentiate between the absence and the presence of 100 and 1000 pg mL^{-1} GFAP by chronoamperometry [20]. A nanocomposite-based antifouling coated electrochemical immunosensor enabling GFAP determination was also reported. The antifouling coating was made of a nanoporous composite material consisting of gold nanowires, carbon nanotubes, and reduced graphene oxide nanoflakes, and allowed the determination of GFAP in the range of 0.01–10 ng mL^{-1} [21]. Moreover, an organic field-effect transistor (OFET)-based biosensor was reported for the label-free

detection of GFAP with a LOD value of 1 ng mL^{-1} [38]. Table 3 summarizes and compares the features of other electrochemical biosensing methods reported for the determination of GFAP. As it can be observed, the developed bioplatform provides some of the better detectability. As it is discussed in section 3.4, the bioplatform allows the determination of GFAP in particularly challenging real samples involving simple protocols and small sample amount.

On the other hand, other biosensing techniques have been used for the determination of GFAP. Agostini et al. reported an ultrahigh-frequency surface-acoustic-wave lab-on-chip able to detect GFAP at a concentration level of 35 pM (1.75 μg mL^{-1}) [39]. Ma et al. reported a fluorescent sandwich immunoassay using carbon dots modified with GFAP specific antibodies to determine GFAP in spiked human serum samples, reaching a LOD of 25 pg mL^{-1} [40]. Importantly, in addition to require more complex and relatively expensive instrumentation, none of these methods achieved significantly lower LODs than that obtained with the developed immunoplatform nor were applied to real samples. Several commercial ELISA kits are also available for the determination of GFAP that claim LOD values ranging between 10 and 1500 pg mL^{-1}, and with test times ranging from 60 to 240 min). Interestingly, the ELISA kit that uses the same immunoreagents that in the developed immunoplatform, recommends the lowest concentration of GFAP standard to be prepared and detected of 313 pg mL^{-1} which is almost 5 times greater than the LOD value calculated for the developed immunoplatform. Moreover, the ELISA method requires relatively costly equipment (ELISA plate readers) hardly portable and miniaturized. Furthermore, available automated commercial methods such as Simoa® (Quanterix) and the prototypes i-STAT™ (Abbott) and ARCHITECT® (Abbott), that claim to measure GFAP between 20 min and 3 h 30 min and reach LOD values ranging between 0.2 and 15 pg mL^{-1} [41]. Despite the high sensitivity of these methods, the methodology reported in this work is suitable for the determination of GFAP and allows it to be carried out at an affordable cost and in decentralized environments.

3.3. Selectivity

The readouts of the developed immunoplatform in the presence of some potential interfering compounds existing in human fluids was studied. The amperometric signal for 0.0 (B) and 7.8 ng mL^{-1} GFAP standards made in the absence and in the presence of 5 mg mL^{-1} human serum albumin (HSA), 10 mg mL^{-1} bovine serum albumin (BSA), 10 ng mL^{-1} S100 calcium-binding protein ß (S100β), 5 mg mL^{-1} hemoglobin (Hb), and 0.01 mg mL^{-1}, 0.1 mg mL^{-1} and 1.0 mg mL^{-1} human immunoglobulin (hIgG) were recorded. Fig. 3 shows that although it is possible to detect GFAP in the presence of all the tested interferents,

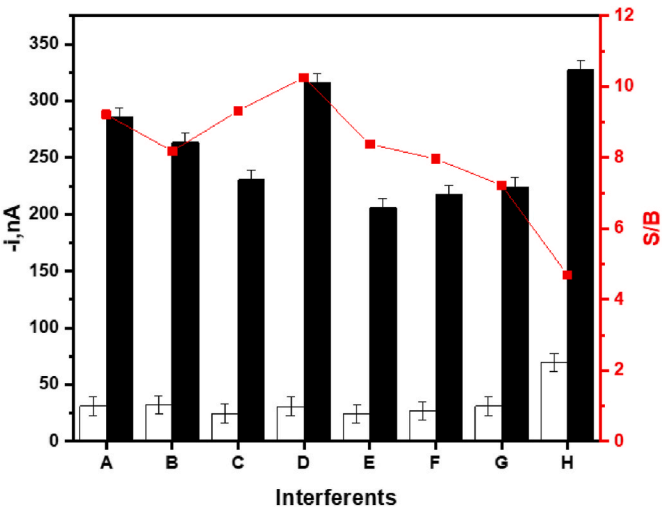


Fig. 3. Amperometric signals recorded with the developed immunoplatform for 0 (B, white bars) and 7.8 ng mL^{-1} (S, black bars) GFAP and the corresponding S/B ratio, red squares and line, in the absence (A) and in the presence of: (B) 10 mg mL^{-1} bovine serum albumin (BSA), (C) 10 ng mL^{-1} S100 calcium-binding protein ß (S100β), (D) 5 mg mL^{-1} human serum albumin (HSA), (E) 0.01 mg mL^{-1}, (F) 0.1 mg mL^{-1}, (G) 1.0 mg mL^{-1} human immunoglobulin (hIgG) and (H) 5 mg mL^{-1} hemoglobin (Hb). (For interpretation of the references to colour in this figure legend, the reader is referred to the Web version of this article.)

both hIgG (G bars) and Hb (H bars) significantly alters the S/B ratio. The effect provoked by hIgG can be attributed to the presence of human antibodies present that reacts with animal proteins (human anti-animal antibodies, HAAA), which can coexist with hIgG and bind epitopes on the Fc portion of foreign immunoglobulins [42]. The larger signals obtained when Hb is the present in the solution may be explained by its intrinsic peroxidase activity [43]. In addition, according to the DY52594-05 DuoSet® ELISA specifications, proteins such as lamin B1, menin, presenilin-1 N-terminal fragment, S100A1, and S100B do not exhibit cross-reactivity with the antibodies involved in the immunoplatform when assayed 200 ng mL^{-1}.

3.4. Analysis of brain tissue extracts

The immunoscaffold was faced to the determination of the endogenous GFAP content in brain tissue protein extracts from healthy individuals and patients diagnosed with dementia. Such individuals were

Table 3
Main features of electrochemical biosensing methods reported for the determination of GFAP.

Methodology	Technique	Linear range	LOD	Sample	Ref.
Immobilization of anti-GFAP CAb on Au electrodes modified with dithiobis(succinimidyl propionate) self-assembled monolayers	EIS	1–10^5 pg mL^{-1}	1 pg mL^{-1}	–	[18]
A specific anti-GFAP antibody was covalently immobilized on the surface of a polyethylenimine coated graphene screen-printed electrode.	EIS	1–10^5 pg mL^{-1}	–	Artificial CSF and serum	[19]
Sandwich immunoassay in which the CAb is immobilized at the bottom of a microcentrifuge tube. Three printed stainless-steel pins (one of them made of carbon ink) act as reference and counter and working electrodes, respectively.	Cronoamperometry	100–1000 pg mL^{-1}	–	–	[20]
Sandwich immunoassay performed on a nanocomposite of BSA interlaced with conductive nanomaterials, Au nanowires, carbon nanotubes, and reduced graphene oxide nanoflakes immobilized on gold electrodes	CV	0.01–10 ng mL^{-1}	–	–	[21]
Screen-printed carbon electrodes modified with a GFAP-imprinted polymer film	DPV	0.2–10 μg mL^{-1}	0.04 μg mL^{-1}	Spiked serum	[37]
Immobilization of a specific anti-GFAP antibody on an organic field effect transistor modified with a polystyrene-co-methacrylic acid layer	FET	1–100 ng mL^{-1}	1 ng mL^{-1}	–	[38]
Sandwich immunoassay performed on the surface MBs magnetically captured on the surface of carbon screen-printed electrodes	Amperometry	0.24–31.6 ng mL^{-1}	67 pg mL^{-1}	Brain tissue extracts	This work

BSA: bovine serum albumin; CA: chronoamperometry; CAb: capture antibody; CSF: cerebrum spinal fluid; CV: cyclic voltammetry; DPV: differential pulse voltammetry; EIS: electrochemical impedance spectroscopy; FET: field-effect transistor; GFAP: glial fibrillary acidic protein, MBs: magnetic microbeads.

classified as: pool of non-demented control subjects (Pool Control), patients diagnosed with vascular dementia (VD) or Alzheimer's disease (AD Braak IV, AD Braak V, and AD Braak VI) and pools (prepared by combining samples from 4 patients diagnosed with the disease at the same Braak stage) of AD patients (Pool AD Braak IV, and Pool AD Braak V).

The amount of brain tissue extract needed to carry out the determination was checked through the comparison of the amperometric recordings obtained for the control subjects and the AD Braak V patients pool using extract amounts between 6.25 and 500 ng. The results displayed in Fig. 4a showed that the smaller amounts of brain tissue extract allowed a better discrimination (AD/H ratio) between the AD Braak V patients and the healthy individuals. Therefore, 6.25 ng was selected to perform the GFAP determination in the selected samples. The potential matrix effect existing in the raw extracts was tested by means of the standard additions method using 6.25 ng of protein tissue extract spiked with increasing concentrations of GFAP standard solutions (5–25 ng mL^{-1}). The comparison between the slope values of the linear calibration plots prepared with GFAP standards (45 ± 2 nA mL ng^{-1}) and the standard additions calibration plot (50 ± 3 nA mL ng^{-1}) showed no significant differences ($t_{exp} = 0.903 < t_{tab} = 4.303$), thus concluding that no apparent matrix effect was observed using such extract amount.

Accordingly, the determination of GFAP was performed by interpolation of the amperometric readings measured for 6.25 ng of protein brain extracts into the calibration plot built with GFAP standards. Fig. 4d displays representative amperograms from the control group (in orange) and the AD V pool (in black). As depicted in Fig. 4b, GFAP levels were significantly higher in samples from AD patients and in AD pool samples than in samples of the healthy individuals pool, in agreement with that reported in the literature [4,6,12]. The significantly lower signal obtained for sample AD Braak V can be explained due to the heterogeneity among individuals. Additionally, the VD patient also exhibited a larger GFAP concentration than the control patient pool as it was previously reported by analyzing CSF [11]. Table 4 summarizes the obtained data for the determination of GFAP using the developed immunoplatform together with the results obtained provided with the ELISA methodology involving the same immunoreagents and according to the protocol described in section 2.6. The statistical comparison in Table 4 shows as $t_{exp} < t_{tab} = 2.776$ in 6 of the 8 samples. In addition, the correlation plot displayed in Fig. 4c has a slope value of (0.9 ± 0.1) and an intercept of (0.0 ± 0.6); $R^2 = 0.996$) which confirmed the great correlation between the results provided with both methodologies despite the high complexity of the analyzed samples. Thus, these results show the competitiveness of the developed methodology to quantify the GFAP

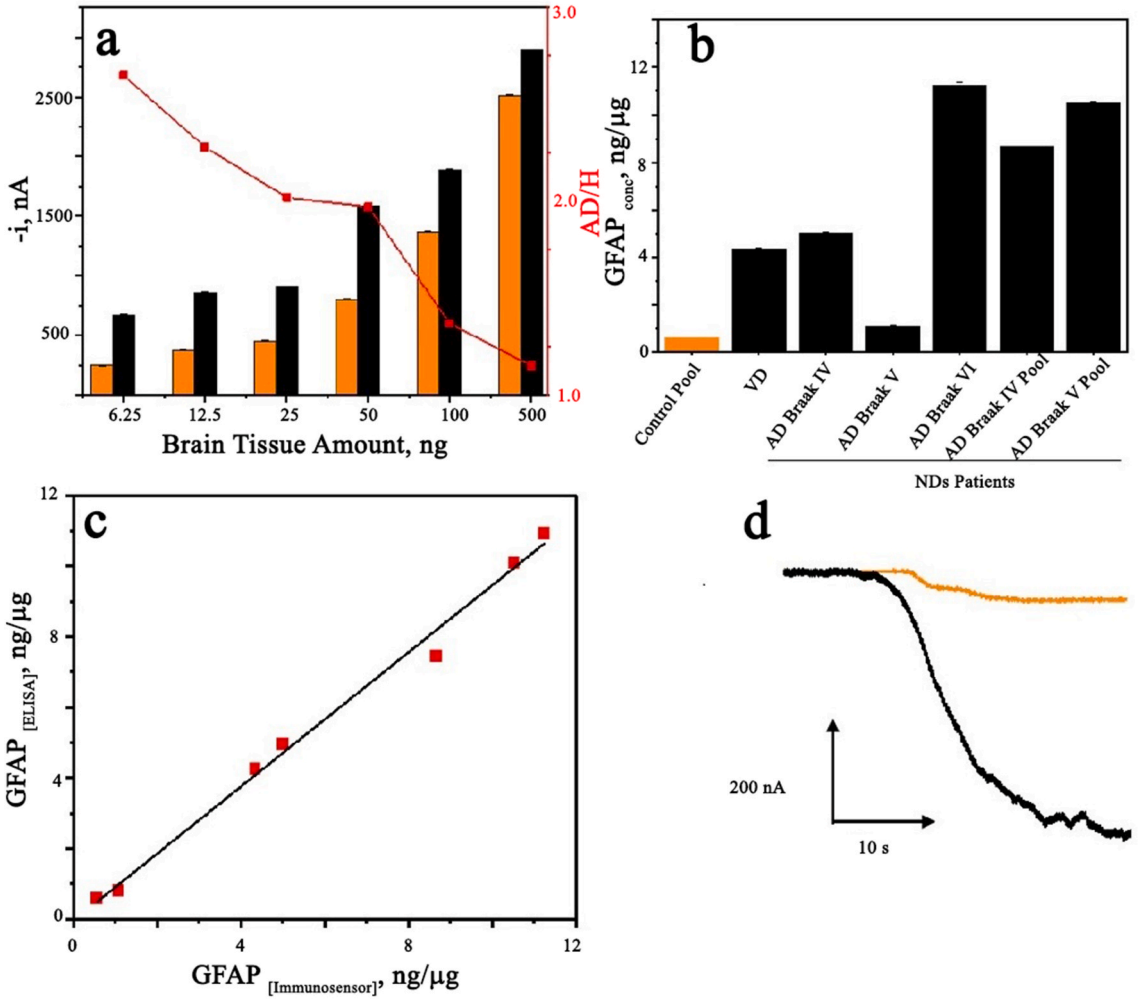


Fig. 4. a) Comparison of the amperometric responses obtained with the developed immunoplatform using different amounts of brain tissue extracts from the healthy control group (orange bars) and AD Braak V patients (black bars) pools; the AD/healthy ratios (AD/H) are shown as red squares and line; b) GFAP concentration values obtained in the analysis of 6.25 ng of brain tissue extracts (numerical values are summarized in Table 4); c) correlation plot between the GFAP concentration values obtained using the developed immunoplatform and the ELISA methodology; real amperometric traces recorded with the immune platform for the control (orange curve) and AD Braak V (black curve) pools. (For interpretation of the references to colour in this figure legend, the reader is referred to the Web version of this article.)

Table 4
Determination of the endogenous GFAP concentration (in ng μg-1) in brain tissue protein extracts from healthy controls and NDs patients (both individual and pools).

Sample	MBs-based immunoplatform		ELISA		t_{exp}
	[GFAP]*	RSD, %	[GFAP]*	$RSD_{n=3}$, %	
Healthy Control Pool	0.56 ± 0.01	4.9	0.58 ± 0.03	8.2	0.591
VD	4.3 ± 0.2	8.4	4.2 ± 0.1	3.4	0.445
AD Braak IV	5.0 ± 0.2	5.4	5.0 ± 0.3	11.0	0.151
AD Braak V	1.06 ± 0.05	7.8	0.82 ± 0.01	1.2	5.208
AD Braak VI	11.2 ± 0.5	7.2	10.9 ± 0.2	3.2	0.601
AD Braak IV Pool	8.7 ± 0.1	1.6	7.5 ± 0.1	2.5	8.900
AD Braak V Pool	10.5 ± 0.1	2.0	10.1 ± 0.2	2.8	2.159

*mean value ± $t \times s/\sqrt{n}$; RSD, %, n = 3, α = 0.05; VD: vascular dementia; AD: Alzheimer's disease.

content in this type of samples using only 6.25 ng of crude extract and within 2 h.

4. Conclusions

A novel MBs-based amperometric immunoplatform is developed to determine GFAP as promising tool for assisting the diagnosis of neurological diseases. The immunoplatform implies an enzyme-labeled sandwich immunoassay with a specific GFAP capture antibody and a biotinylated detector antibody conjugated with Strep-HRP, and amperometric transduction using disposable SPCEs. The developed immunoplatform achieves a LOD of 67 pg mL^{-1} in a s short analysis time (2 h). The immunoplatform can discriminate healthy individuals from patients with AD and VD by interrogating GFAP endogenous levels in protein extracts of post-mortem brain tissues. The obtained results agree with those provided with the ELISA. However, in comparison with the long-established ELISA methodology, developed and validated for the analysis of cell culture supernatants, serum, and plasma samples, the immunoplatform implies a lower-cost methodology and would be compatible with point-of-care use if samples of a less invasive nature were analyzed opening the door to the diagnosis and follow-up of these patients even independently of health institutions. In addition, this bioplatform would allow the identification of post-mortem Alzheimer's disease patients among different types of dementia patients.

Author contribution

Göksu Ozcelikay: Methodology, Investigation, Writing - Review & editing-original draft. **María Gamella**: Methodology, Investigation, Writing - Review & editing-original draft. **Mehmet Altay Unal**: Methodology, Investigation, Review & editing-original draft. **Kıvılcım Gucuyener**: Methodology, Investigation, Review & editing-original draft. **Ana Montero-Calle**: Investigation, Resources, Review & editing original draft. **Rodrigo Barderas**: Conceptualization, Supervision, Resources, Review & editing original draft, Funding acquisition. **José M. Pingarrón**: Supervision, Resources, Review & editing original draft. **Susana Campuzano**: Conceptualization, Supervision, Resources, Writing, Review & editing original draft, Funding acquisition. **Sibel A. Ozkan**: Conceptualization, Supervision, Resources, Writing, Review & editing original draft, Funding acquisition.

Declaration of competing interest

The authors declare that they have no known competing financial interests or personal relationships that could have appeared to influence the work reported in this paper.

Acknowledgments

The financial support of PID2019-103899RB-I00 (Spanish Ministerio de Ciencia e Innovación) Research Project, PI17CIII/00045 and PI20CIII/00019 grants from the AES-ISCIII program and the TRANSNANOAVANSENS-CM Program from the Comunidad de Madrid (Grant S2018/NMT-4349) are gratefully acknowledged. G. Ozcelikay acknowledges the financial support given by Ankara University BAP 21L0237001 and 19B0237004 for her PhD thesis project. Thanks are expressed to TUBITAK for grant support to G. Ozcelikay for a scientific stay in the Complutense University, Faculty of Chemistry, GEBE Research Group.

Appendix A. Supplementary data

Supplementary data to this article can be found online at https://doi.org/10.1016/j.talanta.2022.123526.

References

[1] L.M. Osborn, W. Kamphuis, W.J. Wadman, E.M. Hol, Astrogliosis: an integral player in the pathogenesis of Alzheimer's disease, Prog. Neurobiol. 144 (2016) 121–141, https://doi.org/10.1016/j.pneurobio.2016.01.001.
[2] J.M.A. MacLin, T. Wang, S. Xiao, Biomarkers for the diagnosis of Alzheimer's disease, dementia Lewy body, frontotemporal dementia and vascular dementia, Gen. Psychiatry. 32 (2019) 5–13, https://doi.org/10.1136/gpsych-2019-100054.
[3] C.R. Jack, D.A. Bennett, K. Blennow, M.C. Carrillo, B. Dunn, S.B. Haeberlein, D. M. Holtzman, W. Jagust, F. Jessen, J. Karlawish, E. Liu, J.L. Molinuevo, T. Montine, C. Phelps, K.P. Rankin, C.C. Rowe, P. Scheltens, E. Siemers, H.M. Snyder, R. Sperling, C. Elliott, E. Masliah, L. Ryan, N. Silverberg, NIA-AA Research Framework: toward a biological definition of Alzheimer's disease, Alzheimer's Dementia 14 (2018) 535–562, https://doi.org/10.1016/j.jalz.2018.02.018.
[4] P. Chatterjee, S. Pedrini, E. Stoops, K. Goozee, V.L. Villemagne, P.R. Asih, I.M. W. Verberk, P. Dave, K. Taddei, H.R. Sohrabi, H. Zetterberg, K. Blennow, C. E. Teunissen, H.M. Vanderstichele, R.N. Martins, Plasma glial fibrillary acidic protein is elevated in cognitively normal older adults at risk of Alzheimer's disease, Transl. Psychiatry 11 (2021) 1–10, https://doi.org/10.1038/s41398-020-01137-1.
[5] E.M. Reiman, Y.T. Quiroz, A.S. Fleisher, K. Chen, C. Velez-Pardo, M. Jimenez-Del-Rio, A.M. Fagan, A.R. Shah, S. Alvarez, A. Arbelaez, M. Giraldo, N. Acosta-Baena, R.A. Sperling, B. Dickerson, C.E. Stern, V. Tirado, C. Munoz, R.A. Reiman, M. J. Huentelman, G.E. Alexander, J.B. Langbaum, K.S. Kosik, P.N. Tariot, F. Lopera, Brain imaging and fluid biomarker analysis in young adults at genetic risk for autosomal dominant Alzheimer's disease in the presenilin 1 E280A kindred: a case-control study, Lancet Neurol. 11 (2012) 1048–1056, https://doi.org/10.1016/S1474-4422(12)70228-4.
[6] C. Cicognola, S. Janelidze, J. Hertze, H. Zetterberg, K. Blennow, N. Mattsson-Carlgren, O. Hansson, Plasma glial fibrillary acidic protein detects Alzheimer pathology and predicts future conversion to Alzheimer dementia in patients with mild cognitive impairment, Alzheimer's Res. Ther. 13 (2021) 1, https://doi.org/10.1186/s13195-021-00804-9. –9.
[7] S. Janelidze, N. Mattsson, S. Palmqvist, R. Smith, T.G. Beach, G.E. Serrano, X. Chai, N.K. Proctor, U. Eichenlaub, H. Zetterberg, K. Blennow, E.M. Reiman, E. Stomrud, J.L. Dage, O. Hansson, Plasma P-tau181 in Alzheimer's disease: relationship to other biomarkers, differential diagnosis, neuropathology, and longitudinal progression to Alzheimer's dementia, Nat. Med. 26 (2020) 379–386, https://doi.org/10.1038/s41591-020-0755-1.
[8] J. Lantero Rodriguez, T.K. Karikari, M. Suárez-Calvet, C. Troakes, A. King, A. Emersic, D. Aarsland, A. Hye, H. Zetterberg, K. Blennow, N.J. Ashton, Plasma p-tau181 accurately predicts Alzheimer's disease pathology at least 8 years prior to post-mortem and improves the clinical characterisation of cognitive decline, Acta Neuropathol. 140 (2020) 267–278, https://doi.org/10.1007/s00401-020-02195-x.
[9] A. Nakamura, N. Kaneko, V.L. Villemagne, T. Kato, J. Doecke, V. Doré, C. Fowler, Q.X. Li, R. Martins, C. Rowe, T. Tomita, K. Matsuzaki, K. Ishii, K. Ishii, Y. Arahata, S. Iwamoto, K. Ito, K. Tanaka, C.L. Masters, K. Yanagisawa, High performance plasma amyloid-β biomarkers for Alzheimer's disease, Nature 554 (2018) 249–254, https://doi.org/10.1038/nature25456.
[10] C. Escartin, E. Galea, A. Lakatos, J.P. O'Callaghan, G.C. Petzold, A. Serrano-Pozo, C. Steinhäuser, A. Volterra, G. Carmignoto, A. Agarwal, N.J. Allen, A. Araque, L. Barbeito, A. Barzilai, D.E. Bergles, G. Bonvento, A.M. Butt, W.T. Chen, M. Cohen-Salmon, C. Cunningham, B. Deneen, B. De Strooper, B. Díaz-Castro, C. Farina, M. Freeman, V. Gallo, J.E. Goldman, S.A. Goldman, M. Götz, A. Gutiérrez, P. G. Haydon, D.H. Heiland, E.M. Hol, M.G. Holt, M. Iino, K.V. Kastanenka, H. Kettenmann, B.S. Khakh, S. Koizumi, C.J. Lee, S.A. Liddelow, B.A. MacVicar, P. Magistretti, A. Messing, A. Mishra, A.V. Molofsky, K.K. Murai, et al., Reactive astrocyte nomenclature, definitions, and future, Nat. Neurosci. 24 (2021) 312–325, https://doi.org/10.1038/s41593-020-00783-4.
[11] A. Wallin, K. Blennow, L.E. Rosengren, Glial fibrillary acidic protein in the cerebrospinal fluid of patients with dementia, Dement. Geriatr. Cognit. Disord. 7 (1996) 267–272, https://doi.org/10.1159/000106891.

[12] A.L. Benedet, M. Milà-Alomà, A. Vrillon, N.J. Ashton, T.A. Pascoal, F. Lussier, T. K. Karikari, C. Hourregue, E. Cognat, J. Dumurgier, J. Stevenson, N. Rahmouni, V. Pallen, N.M. Poltronetti, G. Salvadó, M. Shekari, G. Operto, J.D. Gispert, C. Minguillon, K. Fauria, G. Kollmorgen, I. Suridjan, E.R. Zimmer, H. Zetterberg, J. L. Molinuevo, C. Paquet, P. Rosa-Neto, K. Blennow, M. Suárez-Calvet, Differences between plasma and cerebrospinal fluid glial fibrillary acidic protein levels across the alzheimer disease continuum, JAMA Neurol. 78 (2021) 1471–1483, https://doi.org/10.1001/jamaneurol.2021.3671.

[13] L.F. Eng, R.S. Ghirnikar, Y.L. Lee, Glial fibrillary acidic protein: GFAP-Thirty-One years (1969-2000), Neurochem. Res. 25 (2000) 1439–1451, https://doi.org/10.1023/a:1007677003387.

[14] L.E. Pelinka, A. Kroepfl, R. Schmidhammer, M. Krenn, W. Buchinger, H. Redl, A. Raabe, Glial fibrillary acidic protein in serum after traumatic brain injury and multiple trauma, J. Trauma Inj. Infect. Crit. Care 57 (2004) 1006–1012, https://doi.org/10.1097/01.TA.0000108998.48026.C3.

[15] N.A. Huebschmann, T.M. Luoto, J.E. Karr, K. Berghem, K. Blennow, H. Zetterberg, N.J. Ashton, J. Simrén, J.P. Posti, J.M. Gill, G.L. Iverson, Comparing glial fibrillary acidic protein (GFAP) in serum and plasma following mild traumatic brain injury in older adults, Front. Neurol. 11 (2020) 1–12, https://doi.org/10.3389/fneur.2020.01054.

[16] A. Petzold, G. Keir, A.J.E. Green, G. Giovannoni, E.J. Thompson, An ELISA for glial fibrillary acidic protein, J. Immunol. Methods 287 (2004) 169–177, https://doi.org/10.1016/j.jim.2004.01.015.

[17] B. Bellaver, J.P. Ferrari-Souza, L.U. da Ros, S.F. Carter, E. Rodriguez-Vieitez, A. Nordberg, L. Pellerin, P. Rosa-Neto, D.T. Leffa, E.R. Zimmer, Astrocyte biomarkers in alzheimer disease, Neurology 96 (2021) e2944–e2955, https://doi.org/10.1212/WNL.0000000000012109.

[18] S.K. Arya, T.S. Pui, C.C. Wong, S. Kumar, A.R.A. Rahman, Effects of the electrode size and modification protocol on a label-free electrochemical biosensor, Langmuir 29 (2013) 6770–6777, https://doi.org/10.1021/la401109.

[19] S. Khetani, V. Ozhukil Kollath, V. Kundra, M.D. Nguyen, C. Debert, A. Sen, K. Karan, A. Sanati-Nezhad, Polyethylenimine modified graphene-oxide electrochemical immunosensor for the detection of glial fibrillary acidic protein in central nervous system injury, ACS Sens. 3 (2018) 844–851, https://doi.org/10.1021/acssensors.8b00076.

[20] A. González-López, E. Costa-Rama, C. García-Cabo Fernández, L. Benavente-Fernández, S. Calleja-Puerta, B. Fernández-García, R. Pereiro, M.T. Fernández-Abedul, Microcentrifuge tubes as disposable immunoelectrochemical cells for the on-site determination of GFAP, biomarker of hemorrhagic stroke, Proceedings 60 (2020) 10, https://doi.org/10.3390/IECB2020-07060.

[21] S.S. Timilsina, P. Jolly, N. Durr, M. Yafia, D.E. Ingber, Enabling multiplexed electrochemical detection of biomarkers with high sensitivity in complex biological samples, Acc. Chem. Res. 54 (2021) 3529–3539, https://doi.org/10.1021/acs.accounts.1c00382.

[22] I. Weigel, G. Schulze, M. Pischetsrieder, Immunochemical detection of tissue from the central nervous system via myelin proteolipid protein: adaptation for food inspection and development of recombinant bivalent fab mini-antibodies, J. Agric. Food Chem. 58 (2010) 6587–6593, https://doi.org/10.1021/jf100625g.

[23] P.E. Vos, B. Jacobs, T.M.J.C. Andriessen, K.J.B. Lamers, G.F. Borm, T. Beems, M. Edwards, C.F. Rosmalen, J.L.M. Vissers, GFAP and S100B are biomarkers of traumatic brain injury, Neurology 75 (2010) 1786–1793, https://doi.org/10.1212/WNL.0B013E3181FD62D2.

[24] L. Papa, L.M. Lewis, J.L. Falk, Z. Zhang, S. Silvestri, P. Giordano, G.M. Brophy, J. A. Demery, N.K. Dixit, I. Ferguson, M.C. Liu, J. Mo, L. Akinyi, K. Schmid, S. Mondello, C.S. Robertson, F.C. Tortella, R.L. Hayes, K.K.W. Wang, Elevated levels of serum glial fibrillary acidic protein breakdown products in mild and moderate traumatic brain injury are associated with intracranial lesions and neurosurgical intervention, Ann. Emerg. Med. 59 (2012) 471–483, https://doi.org/10.1016/j.annemergmed.2011.08.021.

[25] L. Simani, M. Elmi, M. Asadollahi, Serum GFAP level: a novel adjunctive diagnostic test in differentiate epileptic seizures from psychogenic attacks, Seizure 61 (2018) 41–44, https://doi.org/10.1016/j.seizure.2018.07.010.

[26] C. Muñoz-San Martín, M. Gamella, M. Pedrero, A. Montero-Calle, R. Barderas, S. Campuzano, J.M. Pingarrón, Magnetic beads-based electrochemical immunosensing of HIF-1α, a biomarker of tumoral hypoxia, Sensor. Actuator. B Chem. 307 (2020) 127623, https://doi.org/10.1016/j.snb.2019.127623.

[27] C. Camacho, J.C. Matias, B. Chico, R. Cao, L. Gomez, B.K. Simpson, R. Villalonga, Amperometric biosensor for hydrogen peroxide, using supramolecularly immobilized horseradish peroxidase on the β-cyclodextrin-coated gold electrode, Electroanalysis 19 (2007) 2538–2542, https://doi.org/10.1002/elan.200703993.

[28] D.R. Thal, U. Rüb, M. Orantes, H. Braak, Phases of Aß-deposition in the human brain and its relevance for the development of AD, Neurology 58 (2002) 1791–1800, https://doi.org/10.1212/WNL.58.12.1791.

[29] R. Barderas, I. Babel, R. Díaz-Uriarte, V. Moreno, A. Suárez, F. Bonilla, R. Villar-Vázquez, G. Capellá, J.I. Casal, An optimized predictor panel for colorectal cancer diagnosis based on the combination of tumor-associated antigens obtained from protein and phage microarrays, J. Proteonomics 75 (2012) 4647–4655, https://doi.org/10.1016/j.jprot.2012.03.004.

[30] R. Barderas, R. Villar-Vazquez, M.J. Fernandez-Acenero, I. Babel, A. Pelaez-Garcia, S. Torres, J. Ignacio Casal, Sporadic colon cancer murine models demonstrate the value of autoantibody detection for preclinical cancer diagnosis, Sci. Rep. 3 (2013) 1–7, https://doi.org/10.1038/srep02938.

[31] C.A. Razzino, V. Serafín, M. Gamella, M. Pedrero, A. Montero-Calle, R. Barderas, M. Calero, A.O. Lobo, P. Yáñez-Sedeño, S. Campuzano, J.M. Pingarrón, An electrochemical immunosensor using gold nanoparticles-PAMAM-nanostructured screen-printed carbon electrodes for tau protein determination in plasma and brain tissues from Alzheimer patients, Biosens. Bioelectron. 163 (2020) 1–8, https://doi.org/10.1016/j.bios.2020.112238.

[32] F. Conzuelo, M. Gamella, S. Campuzano, D.G. Pinacho, A.J. Reviejo, M.P. Marco, J. M. Pingarrón, Disposable and integrated amperometric immunosensor for direct determination of sulfonamide antibiotics in milk, Biosens. Bioelectron. 36 (2012) 81–88, https://doi.org/10.1016/j.bios.2012.03.044.

[33] M. Eguílaz, M. Moreno-Guzmán, S. Campuzano, A. González-Cortés, P. Yáñez-Sedeño, J.M. Pingarrón, An electrochemical immunosensor for testosterone using functionalized magnetic beads and screen-printed carbon electrodes, Biosens. Bioelectron. 26 (2010) 517–522, https://doi.org/10.1016/j.bios.2010.07.060.

[34] U. Eletxigerra, J. Martinez-Perdiguero, S. Merino, R. Barderas, V. Ruiz-Valdepeñas Montiel, R. Villalonga, J.M. Pingarrón, S. Campuzano, Estrogen receptor α determination in serum, cell lysates and breast cancer cells using an amperometric magnetoimmunosensing platform, Sens. Bio-Sensing Res. 7 (2016) 71–76, https://doi.org/10.1016/j.sbsr.2016.01.005.

[35] U.D. Teitsdottir, S. Halldorsson, O. Rolfsson, S.H. Lund, M.K. Jonsdottir, J. Snaedal, P.H. Petersen, Cerebrospinal fluid C18 ceramide associates with markers of Alzheimer's disease and inflammation at the pre- and early stages of dementia, J. Alzheimers Dis. 81 (2021) 231–244, https://doi.org/10.3233/JAD-200964.

[36] L.E. Pelika, A. Kroepfl, M. Leixnering, W. Buchinger, A. Raabe, H. Redl, GFAP versus S100B in serum after traumatic brain injury: relationship to brain damage and outcome, J. Neurotrauma 21 (2004) 1553–1561, https://doi.org/10.1089/neu.2004.21.1553.

[37] T. Wang, Y. Fang, Z. He, Electrochemical quantitative detection of glial fibrillary acidic protein based on molecularly imprinted polymer sensor, Int. J. Electrochem. Sci. 12 (2017) 7341–7350, https://doi.org/10.20964/2017.08.69.

[38] J. Song, J. Dailey, H. Li, H.J. Jang, P. Zhang, J.T.H. Wang, A.D. Everett, H.E. Katz, Extended solution gate OFET-based biosensor for label-free glial fibrillary acidic protein detection with polyethylene glycol-containing bioreceptor layer, Adv. Funct. Mater. 27 (2017) 1606506, https://doi.org/10.1002/adfm.201606506.

[39] M. Agostini, F. Amato, M.L. Vieri, G. Greco, I. Tonazzini, L. Baroncelli, M. Caleo, E. Vannini, M. Santi, G. Signore, M. Cecchini, Glial-fibrillary-acidic-protein (GFAP) biomarker detection in serum-matrix: functionalization strategies and detection by an ultra-high-frequency surface-acoustic-wave (UHF-SAW) lab-on-chip, Biosens. Bioelectron. 172 (2021) 112774, https://doi.org/10.1016/j.bios.2020.112774.

[40] Y. Ma, G. Xu, F. Wei, Y. Cen, Y. Song, Y. Ma, X. Xu, M. Shi, M. Sohail, Q. Hu, Carbon dots based immunosorbent assay for the determination of GFAP in human serum, Nanotechnology 29 (2018) 145501, https://doi.org/10.1088/1361-6528/aaabea.

[41] F.K. Korley, S.A. Datwyler, S. Jain, X. Sun, G. Beligere, R. Chandran, J.A. Marino, B. McQuiston, H. Zhang, K.L. Caudle, K.K.W. Wang, A.M. Puccio, D.O. Okonkwo, J. K. Yue, S.R. Taylor, A. Markowitz, G.T. Manley, R. Diaz-Arrastia, Comparison of GFAP and UCH-L1 measurements from two prototype Assays: the abbott i-STAT and ARCHITECT assays, Neurotrauma Rep. 2 (2021) 193–199, https://doi.org/10.1089/neur.2020.0037.

[42] S.E.F. Melanson, M.J. Tanasijevic, P. Jarolim, Cardiac troponin assays: a view from the clinical chemistry laboratory, Circulation 116 (2007), https://doi.org/10.1161/CIRCULATIONAHA.107.722975 e501–4.

[43] D.V. Grigorieva, I.V. Gorudko, A.V. Sokolov, O.V. Kosmachevskaya, A.F. Topunov, I.V. Buko, E.E. Konstantinova, S.N. Cherenkevich, O.M. Panasenko, Measurement of plasma hemoglobin peroxidase activity, Bull. Exp. Biol. Med. 155 (2013) 118–121, https://doi.org/10.1007/s10517-013-2095-3.